PPPL-1992

PPPL--1992

DE83 010838

THEORY OF MODE-INDUCED BEAM-PARTICLE LOSS IN TOKAMAKS

R. B. White, R. J. Goldston, K. McGuire

A. H. Boozer, D. A. Monticello, and W. Park

Plasma Physics Laboratory, Princeton University

P.O. Box 451, Princeton, New Jersey 08544

April, 1983

ABSTRACT

Large-amplitude rotating magnetohydrodynamic modes have been observed to induce significant high-energy-beam particle loss during high-power perpendicular neutral-beam injection on PDX. A Hamiltonian formalism for drift-orbit trajectories in the presence of such modes is used to study induced particle loss analytically and numerically. Results are in good agreement with experiment.

I. INTRODUCTION

Recent results from PDX with near perpendicular high power neutral beam injection[1] indicate that a loss of fast ions takes place when large amplitude high β magnetohydrodynamic (MHD) activity is observed. The MHD activity observed is a mode with poloidal and toroidal mode numbers $m/n = 1/1$ in the plasma core with $m \geq 2$ observed on Mirnov coils inside the vacuum vessel. The Mirnov coils exhibit series of oscillations referred to as "fishbones." These modes are observed to rotate together toroidally at a rate approximately equal to the toroidal precession rate of the injected beam particles. Moderate amplitude fishbone oscillations cause bursts of greatly enhanced, near perpendicular, beam-charge exchange loss in the energy range from half the injection energy up to the injection value. At higher oscillation amplitudes losses of both low energy thermal ions and beam particles with energies well above the injection energy are observed.

In this paper we examine mechanisms for induced particle loss due to rotating MHD modes. In Sec. II the properties and simulation of the fishbone are discussed, and the means by which particles can be ejected is described qualitatively. In Sec. III we review the Hamiltonian formulation of guiding center drifts which we use in our analysis. In Sec. IV the Hamiltonian formalism and Monte Carlo simulations are used to illustrate analytically and numerically the induced particle loss and mode-particle energy transfer during moderate amplitude fishbone oscillations.

Results and implications are summarized in the concluding Sec. V.

II. FISHBONES

The MHD activity of PDX high β discharges (β is the ratio of plasma pressure to magnetic pressure) has been studied using a three-dimensional, high β resistive code HIB.[2,3] This is an initial value code, finite differenced in minor radius and Fourier decomposed in poloidal angle θ and toroidal angle ϕ. The code models PDX as a large aspect ratio device with $\beta \sim O(a/R)$ or smaller. The plasma is assumed to be an incompressible magnetohydrodynamic fluid with scalar resistivity. Diagnostics simulated in the code include magnetic loop signals and soft x-ray signals. The vacuum is modeled by using a highly resistive zero beta plasma.

An initial equilibrium with pressure and current density profiles corresponding to those prevailing during a discharge is used, along with a linearly unstable eigenmode which is predominantly m=1, n=1. Nonlinear development of this eigenmode is followed until the calculated amplitude of the Mirnov coil (magnetic loop) signals reaches the same level as is found in the experiment. The numerically generated wave forms of the Mirnov loop signals and soft x-ray signals agree well with the experimental measurements. Mode frequency is not predicted by this code, and the phase relations of the various modes are only approximate. Plasma rotation, if present, can induce a coupling which would modify the phase relations of the modes from those predicted by our analysis. However, the shape of the simulated Mirnov and soft x-ray signals agrees well with experiment, indicating correct phase relations at least for the large amplitude modes. Typically, it is found that the mode amplitudes decrease rapidly with toroidal mode number n.

Previous work with finite β MHD codes[4] and comparison of the MHD analysis with experiment indicates that the mode, identified as an internal kink, is very near marginal stability. In fact, within the accuracy of the determinations of the pressure and current profiles, it is not known whether the mode is unstable. Thus neither the growth rate of the mode nor its nonlinear saturation value can be predicted from the analysis. The mode structure was studied by choosing the plasma pressure large enough and q on-axis ($q = rB_\phi/RB_\theta$) small enough to make the mode unstable, but another destabilization mechanism would lead to essentially the same harmonic structure. The periodic recurrence of the mode during beam heating suggests that the mode is destabilized by the precessing beam particles, and/or the increased beta produced by the beam. Destabilization by the beam particles might also explain the mode frequency homing on the beam precession frequency. Subsequent ejection of the beam particles by the large amplitude mode, as described in Sec. IV, would then restabilize the mode. The full dynamics of this cycle is beyond the scope of this work, which describes the beam ejection process only.

To study the effect of the mode on the beam particles, the mode spectrum obtained from the code HIB is used in a Monte Carlo code DRIFTS based on the Hamiltonian formalism described in Sec. III. There are several features of particle loss due to fishbone oscillations which can be understood with this formalism:

1. Particle loss due to fishbone activity is a high $\epsilon\beta_p$ phenomenon.
2. During moderate amplitude fishbone oscillations a significant fraction of the energetic beam particles can be lost during a single fishbone period.
3. Although more experiments are necessary to be certain, it appears that particle loss is less severe during parallel neutral beam injection.
4. At moderate mode amplitudes the enhanced loss is in a loss cone typically with $v_\parallel \ll v_\perp$. The energy range is $E \lesssim E_o$, where E_o is the beam injection energy. In some cases particles are also ejected with energies greater than the injection energy. Few low energy thermal ions are expelled.

5. The particles are ejected in a toroidally narrow beacon having a definite phase relation with respect to the rotating mode.
6. At high amplitudes losses of low energy thermal ions are also observed, as well as particles with energies well above the beam injection energy.

All of these points are quantitatively described by our analysis. Here we give a qualitative description of the mechanisms responsible for each of them.

There are three distinct particle loss processes induced by the presence of field perturbations. The first, which we will refer to as mode particle pumping, is a resonance phenomenon, and has no threshold amplitude. As we will see in Sec. IV, significant beam loss is induced only by low m modes which extend to the plasma edge. Analysis with resistive MHD equilibrium codes and the initial value code indicates that the fishbone is primarily a $m=1$, $n=1$ internal kink, and modes with $m>1$ are driven by coupling produced by the outward shift of the magnetic axis, proportional to $\epsilon\beta_p$, where β_p is the poloidal beta. Thus $\epsilon\beta_p$ must be sufficiently large to produce large amplitude low m modes extending to the plasma edge. The amount of particle loss is quantitatively described by rotating low m modes of the amplitude observed with the Mirnov loops.

As will be shown in Sec. IV, the pump mechanism is most effective for near perpendicular beam injection. Only particles with small $V_\parallel$ but with high energy are affected. Thus a loss cone is produced.

It is a property of the pump mechanism that motion of beam particles away from the magnetic axis is correlated with energy decrease. Beam particles are also pumped to higher energies, and radially inward. In the presence of plasma rotation, particles are also ejected with energies significantly higher than the beam injection energy. The pump mechanism has no effect on low energy thermal particles.

Particles are pumped outward only in a narrow toroidal range, producing a beacon of ejected particles correlated with the rotating mode.

The second and third ejection mechanisms are both threshold phenomena and are not related to mode particle pumping. The second mechanism results from the fact that particle orbits are easily modified by magnetic field perturbations in the vicinity of banana tips and, for barely passing particles, near the inside of the torus where the parallel velocity is very small. For banana particles these orbit perturbations can produce stochastic diffusion.[5] For barely passing particles they can produce a transition into the loss cone and immediate loss. The third mechanism involves even higher perturbation amplitudes, where the field itself, and trapped and passing particle orbits, become stochastic. At this point general loss can occur, less correlated with the mode rotation, including loss of thermal particles. In addition, particles previously pumped to higher than injection energies and radially inward by the rotating modes can be lost, producing an efflux of particles with energy significantly higher than the beam injection energy. These latter two processes, which depend critically on a threshold amplitude for the modes, will not be examined quantitatively. If they play a role in particle loss due to fishbones, it can be only for very large amplitudes. Mode particle pumping, however, appears to play an important role in all fishbone oscillations, and to be responsible for the observed saturation of plasma heating. This mechanism will be discussed quantitatively using a moderate amplitude fishbone obtained from the MHD analysis.

III. DRIFT ORBIT HAMILTONIAN

In a recent series of papers a Hamiltonian formalism for guiding center motion in nonaxisymmetric fields has been developed.[6-8] The exact field is assumed to be a perturbation of a nearby field $\vec{B}$, for which exact magnetic surfaces exist. The canonical Hamiltonian variables are closely related to the magnetic coordinates describing this field. Describe $\vec{B}$, in terms of a Clebsch and a covariant representation

$$\vec{B} = \vec{\nabla}\psi \times \vec{\nabla}\theta_o = \vec{\nabla}\chi + \beta^* \vec{\nabla}\psi \ . \tag{1}$$

Here ψ is a magnetic flux coordinate, θ_o measures the angle across the field, and χ the distance along the field. The quantity β^* is related to the plasma current and pressure.

Choose for $\vec{B}$ an axisymmetric equilibrium field in a torus of aspect ratio $\varepsilon^{-1} = R_o/a$. The magnetic coordinates can be expressed in terms of the toroidal coordinates r, θ, and ϕ by equating an expression for $\vec{B}$ in these variables to Eq.(1). In this work we will make use of a pressureless, lowest order in ε equilibrium field,

$$\vec{B} = \frac{r}{q(r)} \vec{\nabla}\phi \times \vec{\nabla}r + R_o\vec{\nabla}\phi \ , \tag{2}$$

where we have normalized $\vec{B}$ to its value on axis. The magnetic coordinates are readily evaluated to any order in ε using higher order expressions for $\vec{B}$.[9] However, in this application finite β plays an important role only in the determination of the modes which are present in the plasma, for which a finite β analysis was used. The beam particle precession frequency is decreased by finite β and predictions of resonant frequencies must take into account this effect, which for PDX is typically a 30% correction. Otherwise plasma pressure is not relevant for a description of the particle motion.

Perturbations of the axisymmetric field due to MHD modes can be represented through $\delta\vec{B} = \vec{\nabla} \times \alpha\vec{B}$ with α a general function of position. This single scalar function is sufficient to represent exactly the radial field perturbation, which dominates the structure of the perturbed magnetic surfaces and is the most important component for the modification of particle orbits.

If α is represented through its Fourier series

$$\alpha = \sum_{m,n} \alpha_{nm}(\psi) \sin (n\phi - m\theta - \omega_{nm} t - \delta_{nm}), \tag{3}$$

the topology of the flux surfaces is changed in the vicinity of a rational surface $q = m/n$ by a magnetic island of width

$$\Delta\psi = 4 \left|\frac{q^2\alpha_{nm}}{\epsilon \; dq/d\psi}\right|^{1/2}. \tag{4}$$

The variable ψ of course does not describe the flux surfaces of the perturbed field, but of the axisymmetric field $\vec{B}$.

The Hamiltonian for the guiding center motion is

$$H = \frac{1}{2} B^2\rho_\parallel^{\,2} + \mu B + \Phi \tag{5}$$

where

$$\rho_\parallel = \frac{v_\parallel}{\omega_c} = (2E - 2\mu B - 2\Phi)^{1/2}/B \tag{6}$$

is the "parallel gyro radius," E is the kinetic energy, Φ the electrostatic potential, and μ the magnetic moment, $\mu = 1/2\, v_\perp^2/B$. Here and in the following we use units with lengths given in terms of the minor radius and time in terms of the on-axis gyro frequency, $\omega_0 = eB_0/mc$. The energy is then given by $E = 1/2\,(\rho/a)^2$ where ρ is the on-axis gyro radius. Here a refers to the tokamak wall, not the plasma edge. In accordance with the MHD simulations the plasma radius was taken to be a/2, leaving a large vacuum region.

The Hamiltonian is a function only of the magnitude of $\vec{B}$. In keeping with the approximate equilibrium used we truncate B to lowest order in ε

$$B = 1 - \varepsilon r \cos\theta. \tag{7}$$

Consistent with this truncation, the canonical variables become

$$\chi = \Phi/\varepsilon, \qquad \rho_c = \rho_\parallel + \alpha\ , \tag{8}$$

$$\theta_o = \theta - \phi/q, \qquad \psi = \frac{r^2}{2}\ , \tag{9}$$

and the guiding center drift equations are

$$\dot{\chi} = \frac{\partial H}{\partial \rho_c}\ , \qquad \dot{\rho}_c = -\frac{\partial H}{\partial \chi}\ , \tag{10}$$

$$\dot{\theta}_o = \frac{\partial H}{\partial \psi}\ , \qquad \dot{\psi} = -\frac{\partial H}{\partial \theta_o}\ .$$

Note that

$$\dot{\rho}_\parallel = \dot{\rho}_c - \frac{\partial \alpha}{\partial \theta_o}\dot{\theta}_o - \frac{\partial \alpha}{\partial \psi}\dot{\psi} - \frac{\partial \alpha}{\partial \chi}\dot{\chi} - \frac{\partial \alpha}{\partial t}\ . \tag{11}$$

The last term, which appears when $\delta\vec{B}$ is explicitly time dependent, represents the forces due to the induced electric field.

The total electric field in the plasma is given by

$$\vec{E} = - \frac{\partial}{\partial t} \alpha \vec{B} - \vec{\nabla}\Phi. \tag{12}$$

The large value of the electron parallel conductivity ensures that the electric field is perpendicular to the magnetic field,

$$(\vec{B} + \delta\vec{B}) \cdot \vec{E} = 0 \tag{13}$$

Writing $\Phi = \Phi_o(\psi) + \Phi_1$ and using $\delta\vec{B} = \vec{\nabla} \times \alpha\vec{B}$, Eq. (13) can be solved for Φ_1, giving

$$\Phi_1 = \sum_{m,n} \frac{\alpha_{nm}[m\Phi_o' + \omega_{nm}]}{\epsilon(n-m/q)} \sin(n\phi - m\theta - \omega t - \delta_{nm}) \tag{14}$$

where the prime refers to differentiation with respect to ψ.

This perturbation solution is singular at the mode rational surfaces, and is incorrect inside the magnetic islands found there. A modification of Φ_1 which avoids these singularities can be introduced through the substitution $(n-m/q)^{-1} \to (n-m/q)((n-m/q)^2 + \delta^2)^{-1}$ with δ chosen to give the island width, i.e., $\delta^2 = 4q'|\alpha_{nm}|/\epsilon$. This ensures approximately correct treatment of the potential within the islands. In addition we have verified, by approaching the ideal limit of zero amplitude at the rational surfaces, that the islands have nothing to do with particle loss. Fishbone oscillations involve only n = 1 and typically only the q = 1 and q = 2 surfaces lie within the plasma, so these island domains represent only a small fraction of the plasma.

Now consider plasma rotation. Particles moving in a potential of the form $\Phi_o(\psi)$ with

$$\Phi_o' = -\frac{\Omega}{q} \tag{15}$$

move as a rigid rotator in the frame moving toroidally with angular rate Ω. The total velocity $\vec{v} = v_\phi\vec{B} + \vec{v}_d$, with $\vec{B}$ given by Eq. (2) and $\vec{v}_d = (\vec{E}\times\vec{B})/B^2$, is $\vec{v} = v_\phi\hat{\phi} + (v_\phi/R - \Omega)(r/q)\hat{\theta}$ giving rigid rotation for a particle with velocity $v_\phi = R\Omega$.

Having chosen the model, i.e., the truncated form of B, the electric potential, and the canonical variables, no approximations may be made in subsequent calculations or energy conservation and the Liouville theorem will not hold. The power of the Hamiltonian formalism consists in the ability to use an approximate model without sacrificing the physically desirable attributes associated with Hamiltonian dynamics.

Energy conserving pitch angle scattering is introduced by changing the pitch $\lambda = V_\parallel/V$ through

$$\lambda' = \lambda(1-\nu\tau) \pm [(1-\lambda^2)\nu\tau]^{1/2} \tag{16}$$

where ν is the collision frequency, τ is the time step with $\nu\tau \ll 1$, and the $\pm$ implies a random sign. This can be shown to give an equivalant Lorentz collision operator.[10]

IV. MODE PARTICLE PUMPING

The guiding center drift equations (10), for $\alpha=0$, describe the trajectories of banana and passing particle orbits in the axisymmetric field

$\vec{B}$. The modes α_{nm} produce perturbations of these orbits which can have periodic and secular parts. We are interested in the latter and in particular in secular modifications of the radial position and of the energy. Consider first the radial position. The radial motion $\dot{\psi}$ is given by

$$\dot{\psi} = -(\rho_{\parallel}^2 B+\mu)\epsilon\, r\sin\theta \tag{17}$$

$$+\sum_{m,n} \frac{m\alpha_{nm}}{\epsilon}\left[\frac{(\omega_{nm} + m\Phi_o')}{(n-m/q)} - \dot{\phi}\right]\cos(n\phi - m\theta - \omega_{nm}t + \delta_{nm})$$

where Eq. (10) has been used to substitute $\dot{\phi}$ for $\epsilon\rho_{\parallel}B^2$.

The radial motion due to α_{nm} can be secular for particles with finite drift excursions, and for trapped particles. The sine term in Eq. (17) is proportional to the square of the gyro radius. It averages to zero when $\alpha = 0$ because of the symmetry of the orbit in θ. For finite perturbation the average of $\sin\theta$ is proportional to α_{nm}. The ratio of the first and second terms is small for typical beam injection parameters and mode frequencies and the $\sin\theta$ term is negligible. The contribution of the cosine term can be obtained by integrating Eq. (17) in time. The only potential considered is that associated with plasma rotation, Eq. (15). In addition, fishbone oscillations consist of co-rotating modes, all with $n = 1$. So, for simplicity, we restrict the modes to $n = 1$ and drop the subscripts on ω_{nm}.

First consider trapped particles. The unperturbed orbit can be approximated by uniform precession in ϕ, $\phi = \Omega t + \omega_p(\psi)t$, and periodic bounce motion in θ, $\theta \approx -\theta_b \sin \omega_b t$. For trapped particles the average toroidal precession rate is given by

$$\omega_p \approx \epsilon\rho^2 q/2r \tag{18}$$

and the bounce frequency by

$$\omega_b \approx \varepsilon\rho\sqrt{\varepsilon r}/q. \tag{19}$$

The variation of ψ in the orbit is an unessential complication and can be neglected. Integrating Eq. (17) over 2k bounces, the average radial motion due to one mode is given by

$$\langle\dot{\psi}\rangle = \frac{A}{4\pi k}\int_{-2\pi k}^{2\pi k} dx \cos\left(\delta_{nm} + bx + z \sin x\right) \tag{20}$$

with $b = (\Omega + \omega_p - \omega)/\omega_b$, $z = m\theta_b$, and

$$A = \frac{m\alpha_{nm}}{\varepsilon}\left(\frac{(\omega - m\Omega/q)}{[1-m/q]} - \omega_p - \Omega\right) \quad . \tag{21}$$

Using the identity

$$e^{iz\sin x} = \sum_{-\infty}^{\infty} J_N(z) e^{iNx} \quad , \tag{22}$$

we then find

$$\langle\dot{\psi}\rangle = \frac{A}{2\pi k}\cos(\delta_{nm})\sin(2\pi kb)\sum_{-\infty}^{\infty}\frac{J_N(z)}{b+N} \qquad b \neq \text{integer}$$

$$\langle\dot{\psi}\rangle = A\cos(\delta_{nm})J_N(z) \qquad b = -N \quad . \tag{23}$$

Secular radial motion occurs only if $b = -N$, integer or equivalently $\omega = \Omega + \omega_p + N\omega_b$. Since typically $\omega_b > \Omega + \omega_p$, the resonance of lowest frequency is the precession frequency resonance, $\omega = \Omega + \omega_p$. The trapped particle precession rate $\omega_p \sim q/r$ is very nearly independent of position for a large range of r, so this condition can be satisfied in much of the plasma. We then find

$$\langle\dot{\psi}\rangle = - \sum_m \cos(\delta_{nm}) \frac{m\alpha_{nm}\omega_p}{\varepsilon(1-nq/m)} J_o(m\theta_b) \quad . \tag{24}$$

The secular motion will be largest for low m and small θ_b. Because of the factor ω_p, the secular motion is proportional to ρ^2 and vanishes in the limit of zero gyro radius.

The particle energy can be treated in a similar manner. Static magnetic and electric fields exactly conserve H, so the change in energy is given by

$$\frac{\partial H}{\partial t} = - \sum \frac{\omega\alpha_{nm}}{\varepsilon} \left[\frac{(\omega + m\Phi_o')}{(n - m/q)} - \dot{\phi}\right]\cos(n\phi - m\theta - \omega t + \delta_{nm}) \; . \tag{25}$$

This expression is similar to that obtained for radial motion, giving for a particle in resonance with the mode

$$\frac{\partial H}{\partial t} = \sum \cos(\delta_{nm}) \frac{\alpha_{nm}\omega^2}{\varepsilon n} \left(1 - \frac{nq}{m}\right)^{-1} J_o(m\theta_b) \quad , \tag{26}$$

Notice that for a single mode $\partial H/\partial t = -(\omega/m)\dot{\psi}$. We thus conclude that particles precessing with the mode in a toroidal position to give outward motion have their energy decreased.

Note that the condition of small $m\theta_b$ implies that significant mode particle pumping occurs only for low q and near perpendicular injection. This is because mode amplitudes are small beyond their associated rational surfaces; and to achieve particle loss, low m modes must extend to the plasma edge. Similarly if the beam injection is not near perpendicular, the particles have large θ_b, so again no pumping occurs. This restriction on θ_b, and hence on parallel velocity, means that ejected particles fill a loss cone with $V_\parallel << V_\perp$. Those modes extending to the plasma edge have mode rational surfaces outside the plasma, and thus $q < m/n$. Eq. (24) then implies that particle mode pumping at the precession frequency will produce a beacon of exiting particles with $|\theta| < \theta_b$ and toroidal ejection point

$$\phi \approx (\omega t - \delta_{nm} + \pi)/n \quad . \tag{27}$$

Note that although it is a resonance phenomenon, and thus requires frequency matching, there is no threshold amplitude for the induced loss.

Now consider passing particles. The average radial motion can again be estimated by substituting the unperturbed orbit in Eq. (17). The relevant drift excursions are those due to θ and ψ. Write $\phi \approx \Omega t + \omega_p t$ and $\theta \approx x - z \sin x$, with $x = \omega_p t/q$, and $z = m\rho/2\psi$, where $\rho = (2E)^{1/2}$ is the gyro radius. The initial pitch, $\lambda = \rho_\parallel/\rho$ is given by

$$\lambda = R_T/\rho \tag{28}$$

where the geometry for the beam injection is shown in Fig. 1, and for particles well into the passing regime, i.e., $R_T/R >> (2\varepsilon r)^{1/2}$, the average toroidal precession is given by

$$\omega_p \approx \varepsilon\rho \frac{R_T}{R} \left[1 - \frac{\varepsilon r R^2}{2R_T^2}\right] . \tag{29}$$

The excursion in ψ is $\psi = \psi_o + \rho \cos x$. The radial motion again takes the form

$$\dot{\psi} = A \cos\left(\delta_{nm} + bx + z \sin x\right) \tag{30}$$

with A given by Eq. (19) and

$$b = q\left(1 - \frac{\omega}{\omega_p} + \frac{\Omega}{\omega_p}\right) - m \quad . \tag{31}$$

The relevant behavior of $\dot{\psi}$ can be understood by neglecting the ψ dependence of A. Integrating Eq. (30) over 2k poloidal periods, the average radial motion is given by Eq. (20). Again the radial motion is secular only for $b = -N$, integer, and

$$\langle\dot{\psi}\rangle = - \sum_m \cos(\delta_{nm}) \frac{N\omega_p \alpha_{nm}}{\epsilon(1-nq/m)} J_N\left(\frac{m\rho}{2\psi}\right). \tag{32}$$

The vanishing of this expression for $N = 0$ insures that the secular motion is again proportional to ρ^2, since both ω_p and the Bessel function are proportional to ρ. Again secular motion vanishes for $\rho = 0$. For every m there is a contribution to $\dot{\psi}$ for

$$\omega = \frac{\omega_p}{q} (q - m + N) + \Omega \tag{33}$$

for all integer $N \neq 0$. Since ω_p/q is a decreasing function of radius and $q - m - N$ increasing, a resonance can extend over a wide range of r. Further, since all m can contribute at the same frequency, there can be significant loss. The modes do not extend beyond their rational surfaces, so $q < m$ at positions where $\dot{\psi}$ is significant. Thus from Eq. (33) $N > 0$, and from Eq. (32)

the toroidal location of the particle loss is again given by Eq. (27). The loss will, in general, be smaller than that in the case of trapped particles because of the smaller range of r within which the resonance condition is satisfied.

Inclusion of the ψ dependence of A in these expressions slightly broadens and complicates the form of the resonance without otherwise changing these conclusions. The resonance is also broadened by the trapping of particles moving at nearby frequencies by the mode itself.

Note that Eq. (33) predicts resonant loss at frequencies well below the transit time frequency. A beacon of exiting particles is produced, as in the case of trapped particles. As in the case of trapped particles $\partial H/\partial t = -(\omega_{nm}/m)\dot{\psi}$, so particle loss is associated with a decrease in energy.

The existence of a radial electric field given by Eq. (15) further modifies the particle behavior in that whereas the total energy is decreased during outward motion, the kinetic energy may in fact be increased.

These results are verified by Monte Carlo simulations. To illustrate the basic effects we show results for uniform radial deposition of a monoenergetic beam of 50 keV deuterium into an equilibrium with a safety factor profile varying from 0.8 on-axis to 2.2 at the plasma edge, and linear in ψ. The plasma edge was located at ψ=0.125, or r=0.5. The on-axis toroidal field was taken to be 9 kG, giving an on-axis gyro frequency of $\omega_o = 4.5 \times 10^7$/sec, and an energy in our dimensionless units of $E = 0.5(\rho/a)^2 = 9 \times 10^{-4}$. The collision frequency was taken to be of the form $\nu \sim \nu_o(1 - r^2/r_p^2)$ with r_p the plasma radius. However, on the time scale of the fishbone oscillations, collisions play a very small role. The static plasma potential Φ_o was taken to be zero except for the investigation of the effect of plasma rotation through the use of the potential given by Eq. (15). The chosen safety factor profile corresponds to that of a moderate amplitude fishbone case. In Fig. 2 are shown the MHD modes used in this simulation. Modes with $m > 0$ were taken to be of the form

$$\alpha_{nm}(\psi) = A\,\psi^{(m/2)}(0.5 - \psi)^P \tag{34}$$

with A, P chosen so that both the maximum value and the value at the rational surface, $q=m/n$, agreed with the values given by the three-dimensional simulation code for a fishbone case. Modes with $n > 1$ are smaller by at least an order of magnitude and were found for this case to have negligible effect on particle confinement and energetics. All low m modes have the same sign, except for $m=0$, which does not contribute to radial pumping. Thus outward pumping is associated with energy decrease for this case.

In Fig. 3 is shown a Poincaré plot, made at $\phi=0$, of the magnetic field produced by these perturbations. The plot extends to the plasma edge. Some degree of stochasticity is observed, but it is not enough to influence energetic ion transport on the time scale of the fishbone oscillations (500 μsec). A factor of 2 increase in these perturbation amplitudes, however, leads to quite a stochastic field, with a Poincaré plot exhibiting few discernable flux surfaces.

In the Monte Carlo simulations the modes were rotated all at the same toroidal rate, as the experiments indicate they do. Plasma rotation is taken to be zero unless otherwise noted.

The resonant behavior of the induced particle loss and energy transfer for near perpendicular injection is clearly seen in Fig. 4. The observed experimental mode frequency for $R_T = 36$ cm is approximately 20 kHz, corresponding to $\omega/\omega_0 = 2.8 \times 10^{-3}$, which is also the precession frequency of particles near the beam injection energy. The effectiveness of this process in expelling a significant fraction of a beam with an energy spread would depend on the ability of the mode to synchronize itself with the bulk of the beam population. In this way, as particles were lost, the mode would shift its frequency to continue work on the remaining beam particles. There is some evidence of frequency modulation of this nature occurring in the experiments.

This figure also shows the effect of variation in the beam injection angle. As R_T is increased, the increased value of θ_b makes the ejection mechanism less effective. As long as the beam consists of trapped particles, the resonant frequency is independent of R_T. The resonance is broader and the losses smaller when the beam consists of passing particles, $R_T > 100$ cm. Particles are lost only from the outer half of the plasma due to the position-dependent resonance condition, Eq. (33). In this region $q \approx 1.5$ and the resonance condition is $N = m-1$ or $\omega \approx \omega_p/3$, which is approximately the location of the resonances for $R_T = 120$ cm and 140 cm. It should be remembered that ejection is also proportional to mode amplitude, so that correlation of fishbone amplitude with beam injection angle would further affect the dependence of particle loss on R_T.

In Fig. 5 is shown a typical orbit for a particle lost due to mode pumping for $R_T = 36$ cm. The time for this whole process is about 100 μsec. Note that the banana is shifted slightly to positive θ, so that the $\sin\theta$ term in Eq. (17) somewhat retards the ejection.

Particle loss due to mode pumping is a linear function of mode amplitude. For near perpendicular injection the 3/1 mode is responsible for 90% of the particle loss observed. Radial drift is proportional to m, which in addition to the relative smallness of the 2/1 mode near the plasma boundary (see Fig. 2) makes the 3/1 mode more effective. Experimenting with individual modes shows that a 4/1 mode as large as the 3/1 mode is also capable of significant particle expulsion, but a 5/1 mode is not.

For near perpendicular injection the radial injection point of ejected particles has a uniform distribution, i.e., particles are lost from the whole plasma, not simply from the edge. For near parallel injection the loss is more restricted to the outer part of the plasma. The toroidal location of the beacon is shown in Fig. 6, and the location agrees with Eq. (27).

For these mode amplitudes the rate of particle loss at near perpendicular injection, for fixed mode frequency, decreases rapidly with decreasing energy and is more than an order of magnitude reduced at 25 keV. There is thus no appreciable loss of low energy thermal particles due to mode pumping. This is simply because the trapped particle precession frequency is proportional to the energy, so these particles do not resonate with the mode.

In Fig. 7 is shown the energy distribution of all particles averaged over a full fishbone period, at 20 kHz mode frequency for $R_T = 36$ cm. Significant broadening of the energy spectrum, with a maximum of 25% energy increase, is observed. Overall the beam energy has been decreased by 5% and the average neutron production rate has been decreased by 5%. The total neutron production rate is, of course, reduced by an amount reflecting the fraction of the beam lost.

In Fig. 8 is shown the overall energy transfer to the particles as a function of particle energy for fixed frequency and $R_T = 36$ cm. The frequency corresponds to the precession rate at $E = 40$ keV. Total energy transfer corresponds to approximately $\Delta E = -700$ eV per particle for particles in the range 25 keV $< E <$ 50 keV. From Monte Carlo simulations in an axisymmetric plasma the number of beam particles in this range at the onset of the fishbone is $\sim 3 \times 10^{18}$ giving a total transfer of ~ 350 J. Total mode energy in the form of magnetic energy in the rotating harmonics for this case was calculated from the MHD code to be 300 J. This beam energy may represent the energy necessary to drive the mode. Whether or not the mode is beam driven is a question which must await a full calculation of the coupled beam and plasma system, as well as sufficiently accurate current density and pressure profile measurements to determine how close the MHD state is to marginal stability.

In Fig. 9 is shown the energy distribution of exiting particles for R_T = 36 cm. As predicted by Eq. (26), particles lost due to mode particle pumping have lost energy, amounting to as much as 20% before exiting. Including plasma rotation through the potential given by Eq. (15) does not produce significantly different results except in the energy distribution of the exiting particles. The total energy distribution is unchanged because of the balance between particles moving inward and those moving outward. The resonance frequency shifts an amount equal to the plasma rotation frequency. In Fig. 9 is also shown the energy distribution of exiting particles for R_T = 36 cm and a plasma rotation frequency of half the mode frequency. A significant high energy population is present, with energies up to 17% above injection energies. It is, however, not clear that this mechanism is sufficient to explain the very high energy particles observed in some fishbone events.[1]

V. CONCLUSION

A mode particle resonance capable of ejecting near perpendicularly injected beam particles has been examined with a Monte Carlo drift orbit code. The mechanism produces a beacon of exiting beam particles correlated with the mode rotation. It appears to be effective enough to explain the loss of beam ions and the saturation of plasma heating observed in PDX during injection because it strongly affects trapped particles with small bounce angle. For fixed mode amplitude the particle loss is not negligible even for parallel injection. How effective the loss mechanism is for nonperpendicular injection therefore depends on whether the fishbone amplitude is large for these cases. The loss mechanism ejects particles with energies lower than the injection energy, except in the presence of plasma rotation, in which case a high energy tail is produced with energies significantly above the injection energy. The energy transfer observed with the drift orbit code indicates that the trapped particles could participate significantly in the destabilization of the mode. The MHD initial value code indicates that the plasma is marginally stable within the accuracy of the determination of the current and pressure. It is destabilized by increase in plasma β and by changing q on-axis. Estimation of the destabilization by the trapped particle population is beyond the scope of this work. However, such a mechanism, along with the beam ejection by the large amplitude mode, could very well explain the cycle of fishbone oscillations observed during near perpendicular beam injection.

ACKNOWLEDGMENTS

This work was supported by U. S. Department of Energy Contract No. DE-AC02-76-CHO-3073.

The authors acknowledge useful conversations with M. N. Rosenbluth, H. L. Berk, W. M. Tang, and R. W. Harvey.

REFERENCES

[1]K. McGuire et al., Princeton Plasma Physics Laboratory Report No. PPPL-1946, 1982.

[2]W. Park, D. A. Monticello, and R. B. White, Bull. Am. Phys. Soc. 23, 779 (1978).

[3]W. Park, D. A. Monticello, R. B. White, K. McGuire, and M. F. Reusch, in Proceedings of the U.S.-Japan Workshop on 3-D Studies, Oak Ridge, TN, 1981.

[4]H. R. Strauss, W. Park, D. A. Monticello, R. B. White, S. C. Jardin, M. S. Chance, A. M. M. Todd, and A. H. Glasser, Nucl. Fusion 20, 638 (1980).

[5]R. J. Goldston, R. B. White, and A. H. Boozer, Phys. Rev. Lett. 47, 647 (1981).

[6]R. B. White, A. H. Boozer, and R. Hay, Phys. Fluids 25, 575 (1982).

[7]A. H. Boozer and R. B. White, Phys. Rev. Lett. 49, 786 (1982).

[8]R. B. White, A. H. Boozer, R. J. Goldston, R. Hay, J. Albert, and C. F. F. Karney, in Proceedings of the Ninth International Conference on Plasma Physics and Controlled Nuclear Fusion Research, 1982, IAEA-CN-41/T-3.

[9]R. Hay, R. B. White, D. A. Monticello, and W. Park, Bull. Am. Phys. Soc. 27, 1126 (1982).

[10]A. H. Boozer and G. Kuo-Petravic, Phys. Fluids 24, 851 (1981).

FIGURE CAPTIONS

FIG. 1 The geometry for beam deposition. R_o = 143 cm and a = 80 cm. The plasma radius is 40 cm, and thus at the plasma edge ψ = 0.125.

FIG. 2 Analytic approximations to the n=1 MHD modes for a moderate amplitude fishbone. The mode maximum and the value at the rational surface both agree with the values given by the MHD simulation. Modes with n>1 were appreciably smaller.

FIG. 3 The Poincaré plot of the magnetic field using the mode amplitudes approximating those given by the MHD simulation for a moderate fishbone. The n=1 modes are shown in Fig. 2. Also included were n=2 and n=3 modes, which at this amplitude have no appreciable effect on particle loss or energy.

FIG. 4 The fraction of beam lost during a fishbone period (500 μ sec) for various values of R_T. The value R_T = 140 cm corresponds to parallel injection.

FIG. 5 A typical trajectory for a beam particle lost due to mode pumping. Here R_T = 35cm and the mode frequency is 20 kHz.

FIG. 6 The toroidal distribution of exiting particles. Here the phase of all modes was $\phi_{nm} = -\pi/2$, and thus from Eq. (27) the ejection should occur at $\phi - \omega t = 3\pi/2$. Note that since particle ejection is almost entirely due to the 3/1 mode, the location of the beacon with respect to the 1/1 mode can be tuned by adjusting the relative phase of these modes.

FIG. 7 The particle energy distribution averaged over a full fishbone period. The mode frequency is 20 kHz, $R_T = 35$ cm, and $E_o = 50$ keV. The maximum particle energy amounts to a 16% increase over the injection energy.

FIG. 8 The total energy transfer to a mono-energetic beam from the mode as a function of particle energy. The mode frequency corresponds to the precession rate at 38 keV. Here $R_T = 35$ cm.

FIG. 9 The energy distribution of the ejected particles. The mode frequency is 20 kHz, $R_T = 35$ cm, and the injection energy is $E_o = 9 \times 10^{-4}$, which corresponds to 50 keV. Also shown is a case with a plasma rotation of half the mode frequency.

82T0249

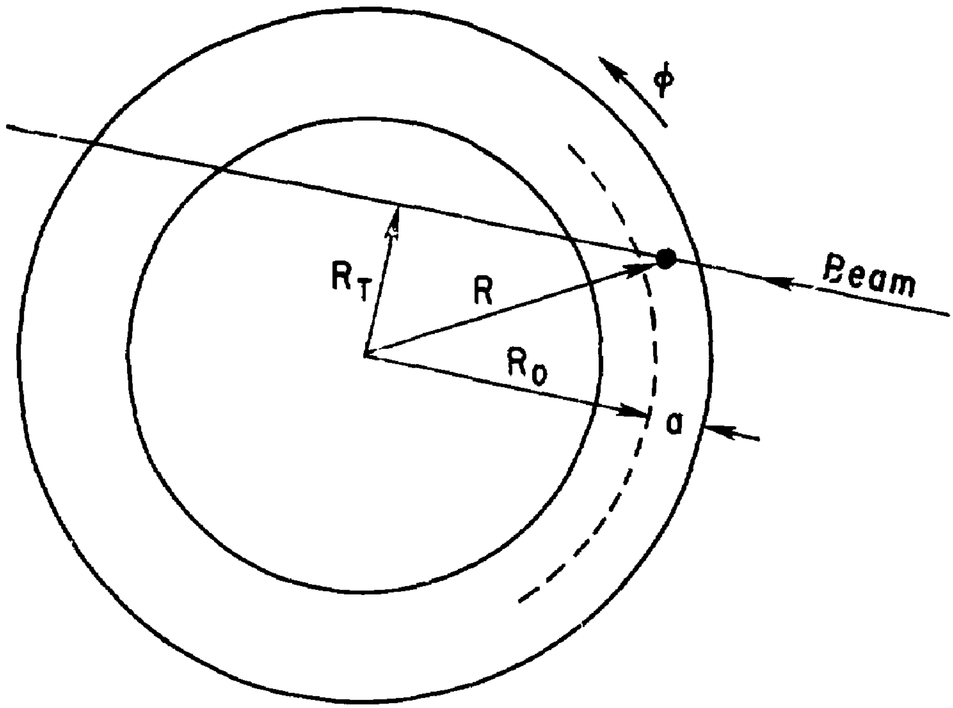

Fig. 1

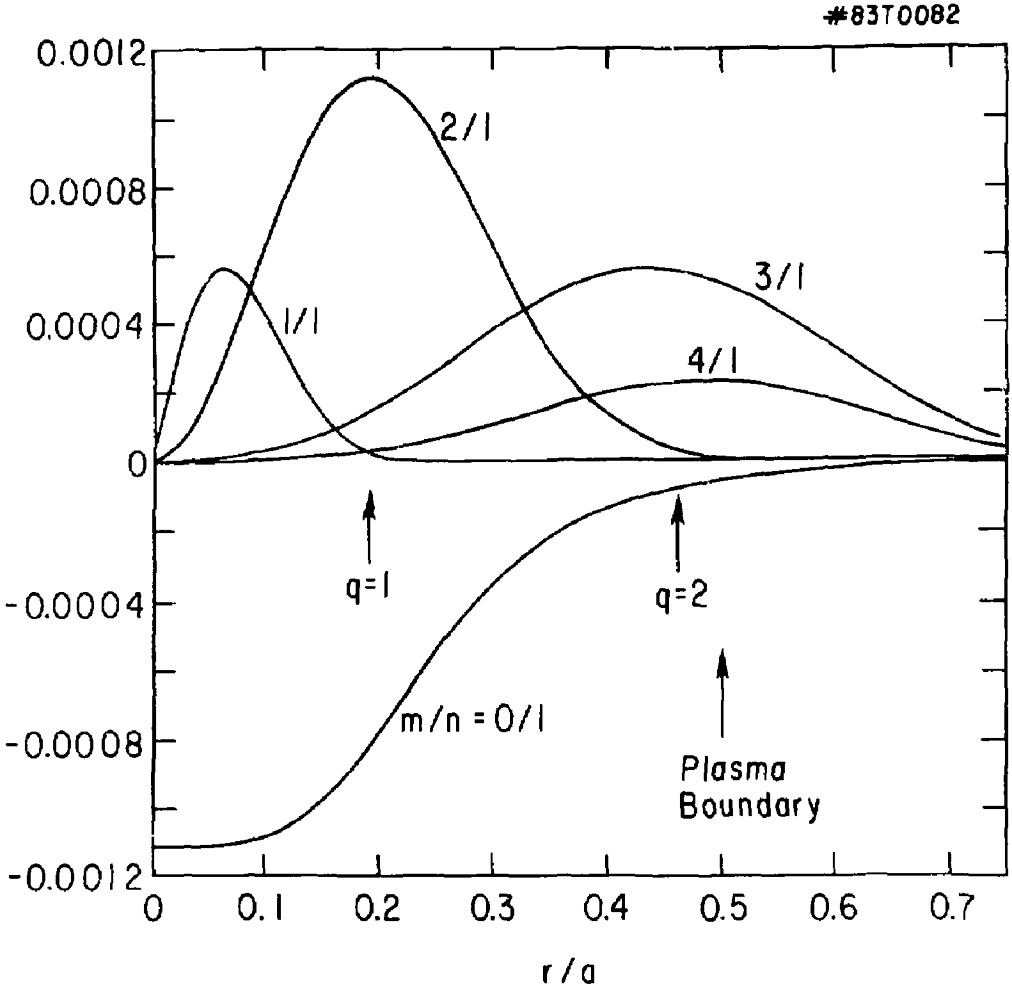
#83T0082
0.0012
0.0008
0.0004
0
-0.0004
-0.0008
-0.0012
0
0.1
0.2
0.3
0.4
0.5
0.6
0.7
r/a
2/1
1/1
3/1
4/1
q=1
q=2
m/n = 0/1
Plasma Boundary

Fig. 2

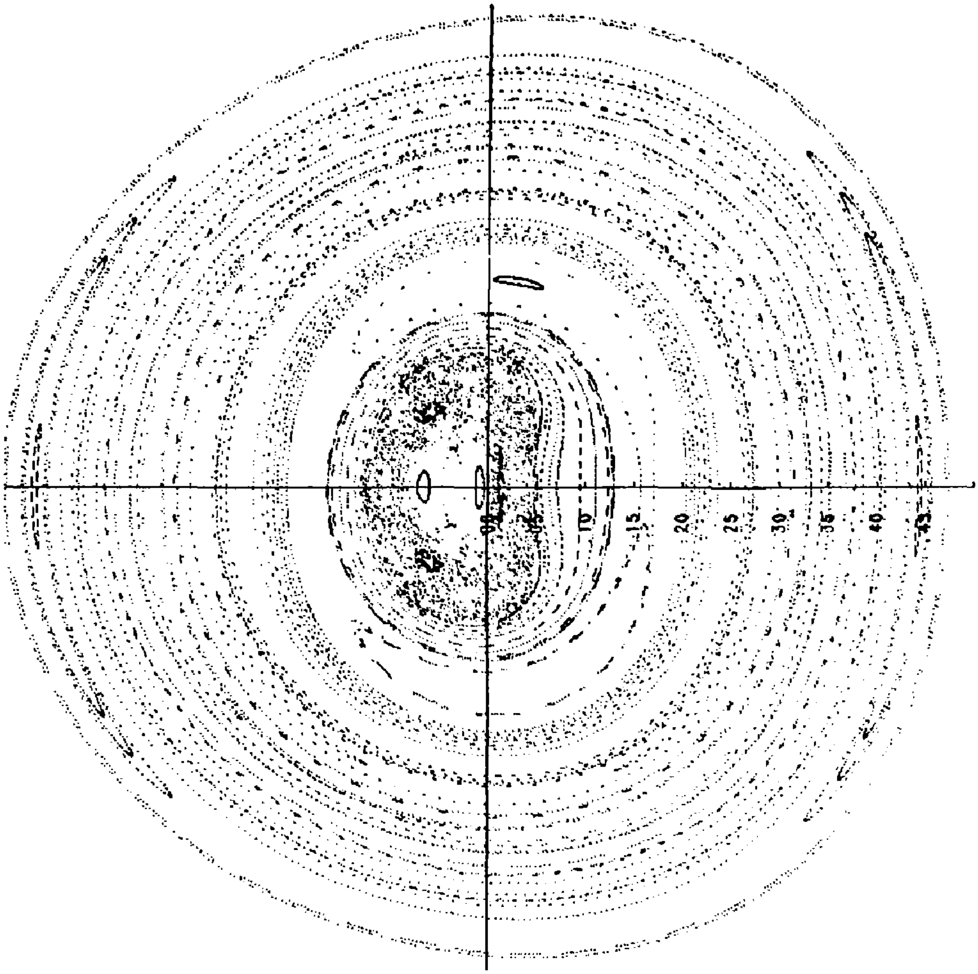

Fig. 3

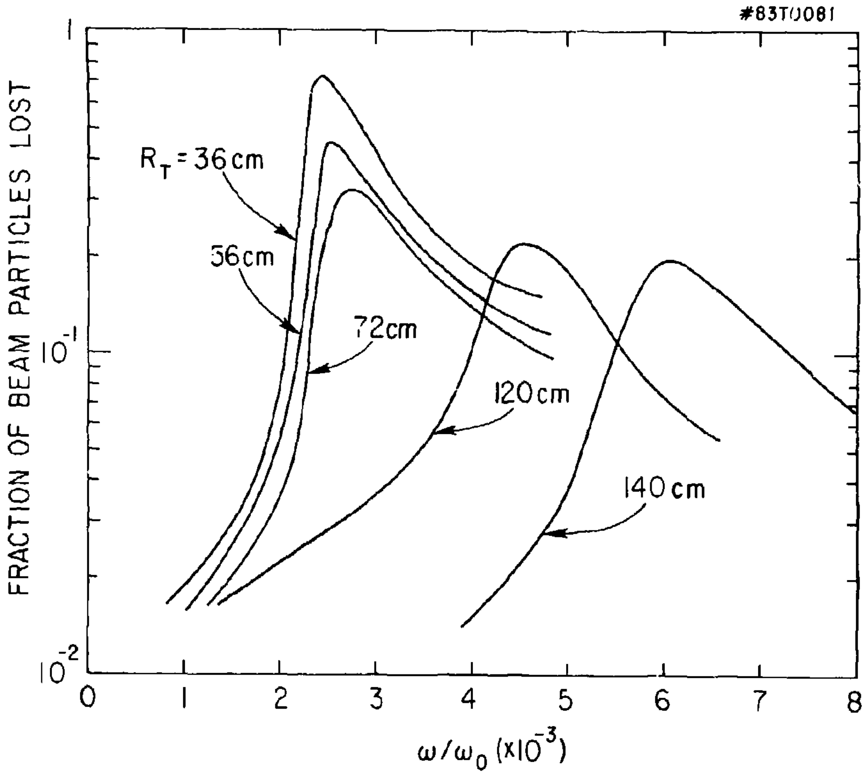
#83T0081
FRACTION OF BEAM PARTICLES LOST
1
10^{-1}
10^{-2}
0
1
2
3
4
5
6
7
8
$\omega/\omega_0\,(\times 10^{-3})$
$R_T = 36$ cm
56 cm
72 cm
120 cm
140 cm

Fig. 4

#83T0083

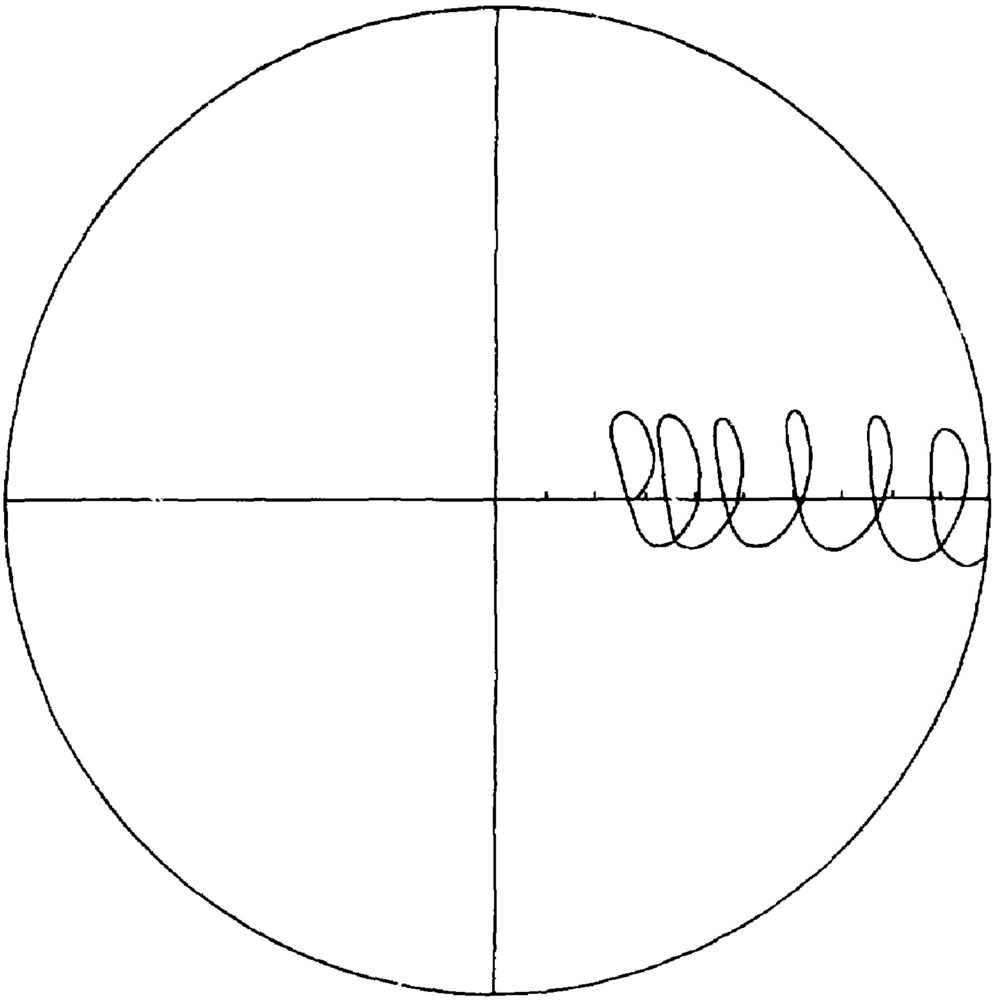

Fig. 5

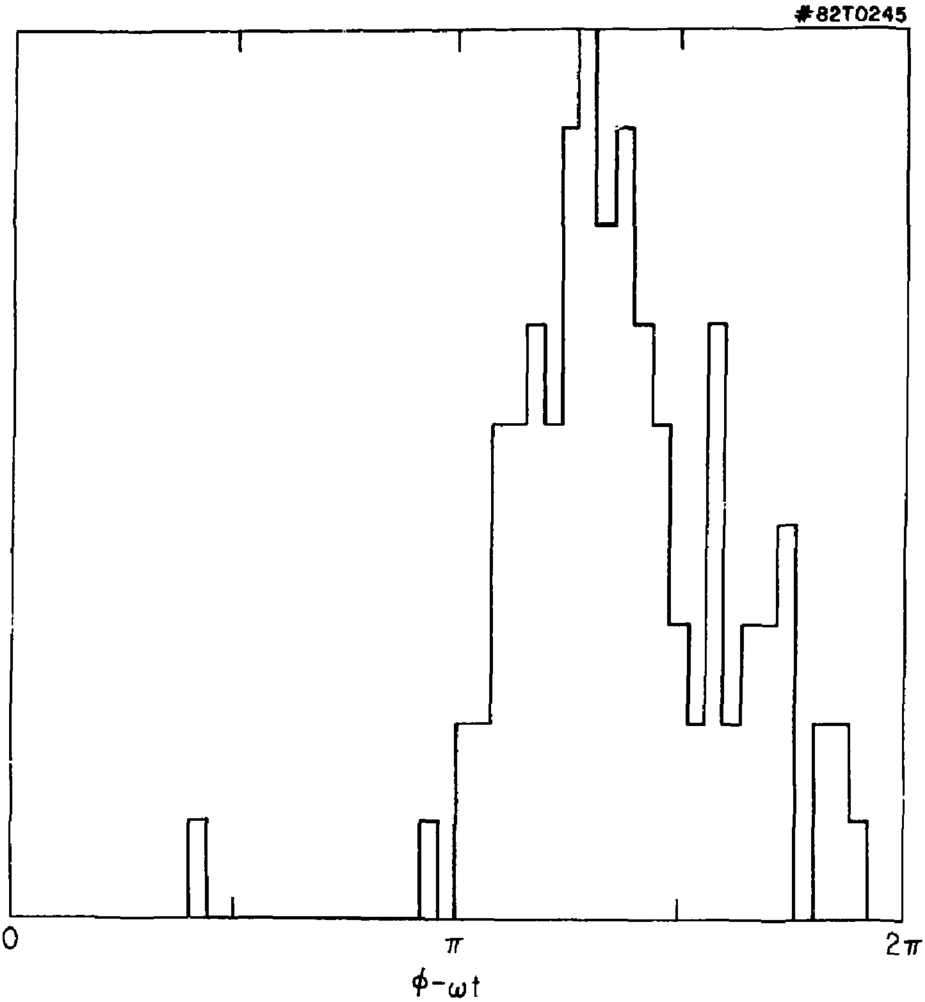

Fig. 6

83T0085

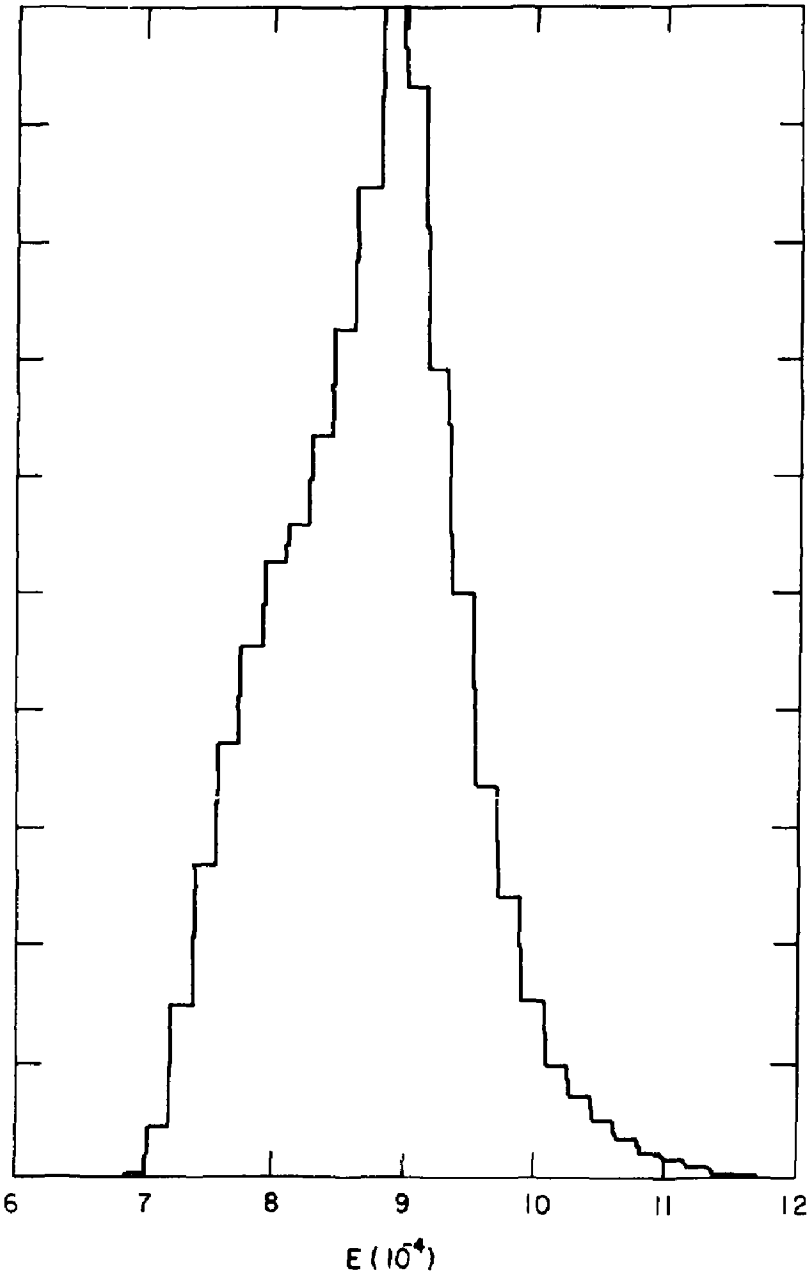

Fig. 7

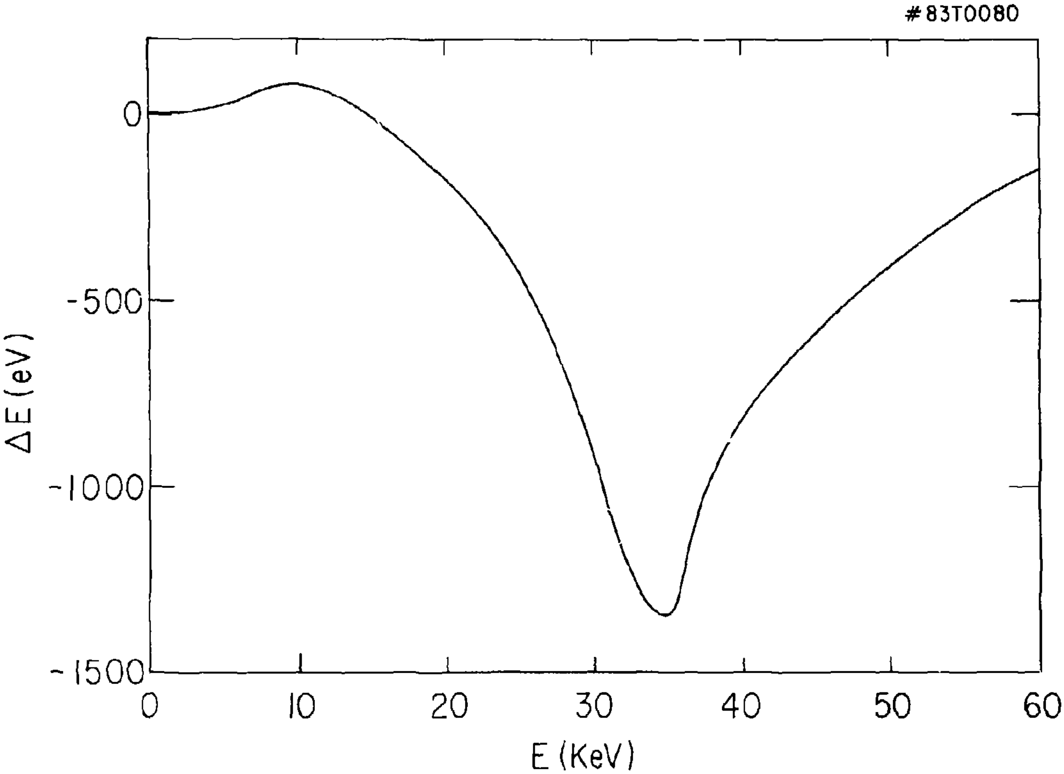

Fig. 8

#83T0084

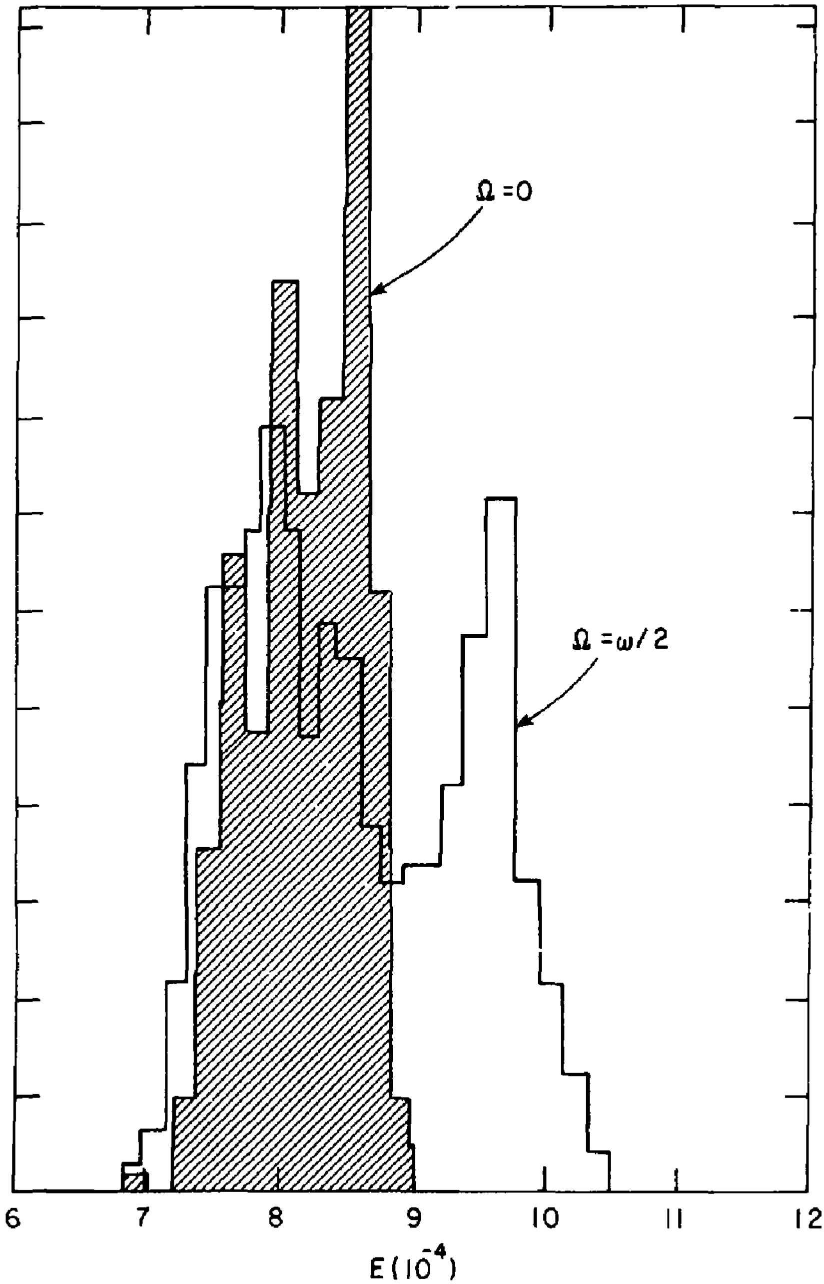

Fig. 9

EXTERNAL DISTRIBUTION IN ADDITION TO TIC UC-20

Plasma Res Lab, Austra Nat'l Univ, AUSTRALIA
Dr. Frank J. Paoloni, Univ of Wollongong, AUSTRALIA
Prof. I.R. Jones, Flinders Univ., AUSTRALIA
Prof. M.H. Brennan, Univ Sydney, AUSTRALIA
Prof. F. Cap, Inst Theo Phys, AUSTRIA
Prof. Frank Verheest, Inst theoretische, BELGIUM
Dr. D. Palumbo, Dg XII Fusion Prog, BELGIUM
Ecole Royale Militaire, Lab de Phys Plasmas, BELGIUM
Dr. P.H. Sakanaka, Univ Estadual, BRAZIL
Dr. C.R. James, Univ of Alberta, CANADA
Prof. J. Teichmann, Univ of Montreal, CANADA
Dr. H.M. Skarsgard, Univ of Saskatchewan, CANADA
Prof. S.R. Sreenivasan, University of Calgary, CANADA
Prof. Tudor W. Johnston, INRS-Energie, CANADA
Dr. Hannes Barnard, Univ British Columbia, CANADA
Dr. M.P. Bachynski, MPB Technologies, Inc., CANADA
Zhengwu Li, SW Inst Physics, CHINA
Library, Tsing Hua University, CHINA
Librarian, Institute of Physics, CHINA
Inst Plasma Phys, SW Inst Physics, CHINA
Dr. Peter Lukac, Komenskeho Univ, CZECHOSLOVAKIA
The Librarian, Culham Laboratory, ENGLAND
Prof. Schatzman, Observatoire de Nice, FRANCE
J. Radet, CEN-BP6, FRANCE
AM Dupas Library, AM Dupas Library, FRANCE
Dr. Tom Mual, Academy Bibliographic, HONG KONG
Preprint Library, Cent Res Inst Phys, HUNGARY
Dr. A.K. Sundaram, Physical Research Lab, INDIA
Dr. S.K. Trehan, Panjab University, INDIA
Dr. Indra, Mohan Lal Das, Banaras Hindu Univ, INDIA
Dr. L.K. Chavda, South Gujarat Univ, INDIA
Dr. R.K. Chhajlani, Var Ruchi Marg, INDIA
B. Buti, Physical Research Lab, INDIA
Dr. Phillip Rosenau, Israel Inst Tech, ISRAEL
Prof. S. Cuperman, Tel Aviv University, ISRAEL
Prof. G. Rostagni, Univ Di Padova, ITALY
Librarian, Int'l Ctr Theo Phys, ITALY
Miss Clelia De Palo, Assoc EURATOM-CNEN, ITALY
Biblioteca, del CNR EURATOM, ITALY
Dr. H. Yamato, Toshiba Res & Dev, JAPAN
Prof. M. Yoshikawa, JAERI, Tokai Res Est, JAPAN
Prof. T. Uchida, University of Tokyo, JAPAN
Research Info Center, Nagoya University, JAPAN
Prof. Kyoji Nishikawa, Univ of Hiroshima, JAPAN
Sigeru Mori, JAERI, JAPAN
Library, Kyoto University, JAPAN
Prof. Ichiro Kawakami, Nihon Univ, JAPAN
Prof. Satoshi Itoh, Kyushu University, JAPAN
Tech Info Division, Korea Atomic Energy, KOREA
Dr. R. England, Civdad Universitaria, MEXICO
Bibliotheek, Fom-Inst Voor Plasma, NETHERLANDS
Prof. B.S. Liley, University of Waikato, NEW ZEALAND
Dr. Suresh C. Sharma, Univ of Calabar, NIGERIA
Prof. J.A.C. Cabral, Inst Superior Tech, PORTUGAL
Dr. Octavian Petrus, ALI CUZA University, ROMANIA
Dr. R. Jones, Nat'l Univ Singapore, SINGAPORE
Prof. M.A. Hellberg, University of Natal, SO AFRICA
Dr. Johan de Villiers, Atomic Energy Bd, SO AFRICA
Dr. J.A. Tagle, JEN, SPAIN
Prof. Hans Wilhelmson, Chalmers Univ Tech, SWEDEN
Dr. Lennart Stenflo, University of UMEA, SWEDEN
Library, Royal Inst Tech, SWEDEN
Dr. Erik T. Karlson, Uppsala Universitet, SWEDEN
Centre de Recherchesen, Ecole Polytech Fed, SWITZERLAND
Dr. W.L. Weise, Nat'l Bur Stand, USA
Dr. W.M. Stacey, Georg Inst Tech, USA
Dr. S.T. Wu, Univ Alabama, USA
Mr. Norman L. Oleson, Univ S Florida, USA
Dr. Benjamin Ma, Iowa State Univ, USA
Magne Kristiansen, Texas Tech Univ, USA
Dr. Raymond Askew, Auburn Univ, USA
Dr. V.T. Tolok, Kharkov Phys Tech Ins, USSR
Dr. D.D. Ryutov, Siberian Acad Sci, USSR
Dr. M.S. Rabinovich, Lebedev Physical Inst, USSR
Dr. G.A. Eliseev, Kurchatov Institute, USSR
Dr. V.A. Glukhikh, Inst Electro-Physical, USSR
Prof. T.J. Boyd, Univ College N Wales, WALES
Dr. K. Schindler, Ruhr Universitat, W. GERMANY
Nuclear Res Estab, Julich Ltd, W. GERMANY
Librarian, Max-Planck Institut, W. GERMANY
Dr. H.J. Kaeppler, University Stuttgart, W. GERMANY
Bibliothek, Inst Plasmaforschung, W. GERMANY